# Numerical Analysis of Free Flow Past a Sluice Gate

By Dae-Geun Kim*

.................................................................................................................................................................................................

## Abstract

Sluice gates are widely used for flow control in open channels. This study shows that numerical tools using the Reynolds averaging Navier-Stokes equations are sufficiently advanced to calculate the contraction and the discharge coefficients, and the pressure distribution for free flow past a sluice gate. The trend of the existing inviscid theoretical contraction coefficient is quite different from existing experiments. As the gate opening rate increases, the contraction coefficient for the present study gradually decreases if the gate opening rate is less than 0.4 and increases when the gate opening rate is larger than 0.4, exhibiting a tendency similar to existing experimental data. This is because energy losses by friction and water surface oscillations increase as the approach velocity from the gate increases as the gate opening rate is larger than 0.4. The discharge coefficients and the pressure distributions from the present analysis correspond closely to the existing experimental data. In this study, by performing a numerical analysis that does not use the assumptions adopted in the existing potential flow theory, the contraction coefficient, the discharge coefficient, and the pressure distributions were thoroughly analyzed. This study shows that existing numerical models using RANS are a useful tool in the design of hydraulic structures.

Keywords: *contraction coefficient, discharge coefficient, RANS, sluice gate*

.................................................................................................................................................................................................

## 1. Introduction

Sluice gates are widely used for controlling discharge and flow depth in irrigation channels, large sewers, and in hydraulic structures. Due to the practical importance of the sluice gate as a control and metering device, the prediction of the flow characteristics under gates was one of the classical problems of hydraulics.

The discharge through a sluice gate is affected not only by the upstream flow depth for free flow but also by both the upstream and downstream flow depths for submerged flow (Henderson, 1966; Lin et al., 2002). Similarly, for a given discharge, the upstream flow depth is independent of the tailwater depth in a free flow, but increases with the tailwater depth when a gate is submerged.

Most features of sluice gate flow seem to be predicted accurately by existing mathematical models based on the potential flow theory, but there remain persistent discrepancies between the theoretical and the experimental values of the contraction coefficient. Due to the existence of boundary layer growth (Benjamin, 1956; Henderson, 1966; Rajaratnam and Subramanya, 1967) and energy losses between the upstream and downstream sections of the gate (Montes, 1997; Roth and Hager, 1999), experimental values of the contraction coefficient always exceed the theoretical values by 5-10%. However, the experimental values of the discharge coefficient, which depend on the separate measurement of the discharge rather than depth, agree better with theory.

The viscous fluid and turbulent flow properties are assumed to be represented sufficiently well by an irrotational inviscid flow. In addition, some early researchers simplified the problem by assuming that the free surface upstream of the gate may be represented by a horizontal, and by neglecting gravitational effects. An extensive review of the existing theoretical research on this field was summarized by Montes (1997). Most existing attempts of modeling gate flow have used potential flow theory and mapping into the complex potential plane (Fangmeier and Strelkoff, 1968; Larock, 1969; Cheng et al., 1981; Masliyah et al., 1985; Montes, 1997; Vanden-Broeck, 1997).

With the advances in computational modeling for solving the governing equations of fluid flow, the numerical solution of the Reynolds averaged Navier-Stokes (RANS) equations using turbulence models is an alternative to analyzing the free flow past a sluice gate. Investigations of flow over ogee-spillways were carried out using a computational fluid dynamics program, FLOW-3D, which solves the RANS equations (Savage and Johnson, 2001). These studies show that there is reasonably good agreement between the physical and numerical models for the water surface profile, the pressure distribution, and discharge. The present study considers the gate flow problem numerically using the RANS equations, where the above schematization is not necessary. By performing a numerical analysis that does not employ the assumptions adopted in the existing potential flow theory, the contraction coefficient, the discharge coefficient, and the pressure distribution were thoroughly analyzed. A commercially available computational fluid dynamics program FLOW-3D, which solves the RANS equations, was used herein. FLOW-3D was widely verified and used in hydraulics. The simulation results are compared with existing theoretical and experimental data.

*Member, Lecturer, Major in Civil Engrg., Division of Construction Engrg., Mokpo National Univ., Muan-Gun, Chonnam 534-729, Korea (E-mail: kdg05@mokpo.ac.kr)

## 2. Theoretical Background

### 2.1 Free Flow past a Sluice Gate

Consider a two-dimensional steady flow past a sluice gate confined to the *x-z* plane of a rectangular Cartesian coordinate system (*x, y, z*). Let the sluice gate be located at *x*=0, as shown in Fig. 1 and the bottom surface be horizontal. In Fig. 1, $h_1$= approach flow depth, $V_1$=approach flow velocity, $E_1$=upstream energy, $h_2$=flow depth at the vena contracta, $V_2$=downstream flow velocity, $E_2$=downstream energy, $h_3$=flow depth sufficiently downstream from the gate, *a*=gate opening, $h_{pg}$=pressure head on the gate, and $\Delta E$=energy loss. The degree of contraction may be represented by the contraction coefficient $C_c$, defined as the ratio of the flow depth at the vena contracta and the gate opening as

$$C_c = \frac{h_2}{a} \tag{1}$$

If $\Delta E$ may be neglected, the discharge through a sluice gate may be expressed with the discharge coefficient, $C_d$ as (Henderson, 1966)

$$q = C_d a \sqrt{2gh_1} \tag{2}$$

where g=gravitational acceleration. A summary of past investigations on the contraction and the discharge coefficients is provided in Tables 1, 2, and 3. In general, the experimental contraction coefficients are somewhat larger that those computed from the potential flow theory. This difference is due to the boundary layer growth and energy losses due to a horseshoe
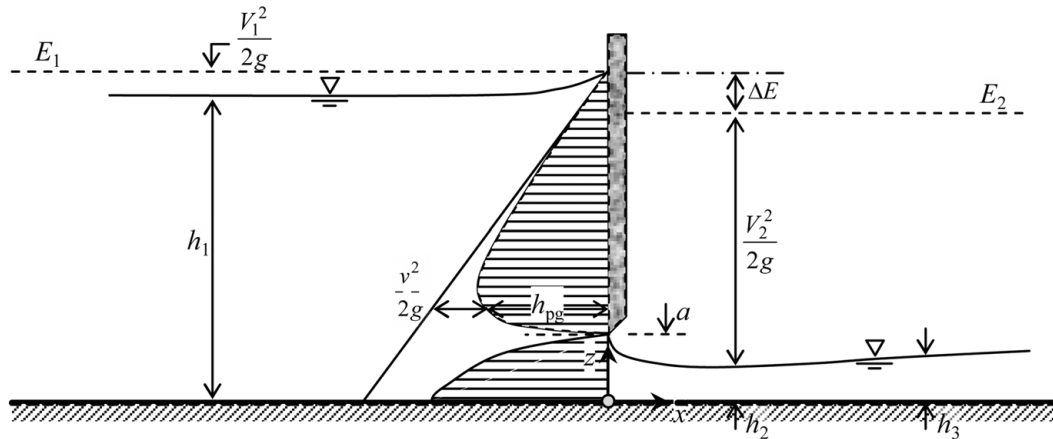


Fig. 1. Definition Plot of Plane Sluice Gate

Table 1. Summary of Previous Theoretical Investigations on the Contraction Coefficient

| Investigation | Assumptions | Range | Remarks |
|---|---|---|---|
| Von Mises (1917) (reported by Henderson (1966)) | NG, IVF, HPFS | 0.611 ~ 0.598 | decreasing as $a/E_1$ increases |
| Benjamin (1956) | IVF, HPFS | 0.611 ~ 0.599 | decreasing as $a/E_1$ increases |
| Perry (1957) (reported by Montes (1997)) | IVF, HPFS | 0.611–(0.017/($E_1/a$–1)) | decreasing as $a/E_1$ increases |
| Chung (1972) | IVF, HPFS | 0.611 ~ 0.590 | decreasing as $a/E_1$ increases |
| Southwell and Vaisey (1946) (reported by Montes (1997)) | IVF | 0.608 | $a/E_1 = 0.53$ |
| Fangmeier and Strelkoff (1968) | IVF | 0.611 ~ 0.593 | decreasing as $a/E_1$ increases |
| Isaacs (1977) | IVF | 0.597 | $a/E_1 = 0.30$ |
| Montes (1997) | IVF | 0.611 ~ 0.604 | decreasing as $a/E_1$ increases |
| Vanden-Broeck (1997) | IVF | 0.611 ~ 0.590 | decreasing as $a/E_1$ increases |

NG: no gravitational effects
IVF: inviscid fluid
HPFS: free surface upstream of the gate is horizontal plane

Table 2. Summary of Previous Experimental Investigations on the Contraction Coefficient

| Investigation | Gate opening (cm) | Range | Remarks |
|---|---|---|---|
| Gibson (1918) (reported by Montes (1997)) | 3.2, 6.3, 9.4 | 0.580 ~ 0.630 | increasing as $a/E_1$ increases |
| Fawer (1937) (reported by Montes (1997)) | 2.0, 3.0, 4.0 | 0.611 ~ 0.599 | increasing as $a/E_1$ increases |
| Benjamin (1956) | 2.6, 9.1 | 0.615 ~ 0.733 | increasing as $a/E_1$ increases |
| Rajaratnam and Subramanya (1967) | 2.6 – 10.1 | 0.580 ~ 0.630 | |
| Roth and Hager (1999) | 5.0 | about 0.595 | increasing as $a/E_1$ increases |
| Lin et al. (2002) | 2.5, 3.5 | 0.590 ~ 0.610 | increasing as $a/E_1$ increases |

Table 3. Summary of Previous Experimental Investigations on the Discharge Coefficient

| Investigation | Gate opening (cm) | Range | Remarks |
|---|---|---|---|
| Rajaratnam and Subramanya (1967) | 2.6-10.1 | 0.595 | increasing slightly as $a/E_1$ increases |
| Nago (1978) (reported by Roth and Hager (1999)) | 6.0 | $0.595 \sim 0.520$ | decreasing as $a/E_1$ increases |
| Roth and Hager (1999) | 5.0 | $0.594 \sim 0.492$ | decreasing as $a/E_1$ increases |

vortex and recirculating zone observed upstream of the gate; hence the water surface profile is raised with respect to the inviscid solution. In an inviscid solution, it is assumed that the flow is irrotational and has constant specific energy. The flow in the real plane is mapped into a rectangular strip in the complex potential plane, which is subdivided into a rectangular grid.

## 2.2 Numerical Modeling

The commercially available CFD package FLOW-3D uses a finite-volume approach to solve the RANS equations by implementing of the Fractional Area/Volume Obstacle Representation (FAVOR) method to define an obstacle (Flow Science, 2002). The general governing RANS and continuity equations for an incompressible flow, including the FAVOR variables, are given by

$$\frac{\partial}{\partial x_i}(u_i A_i) = 0 \tag{3}$$

$$\frac{\partial u_i}{\partial t} + \frac{1}{V_F}\left(u_j A_j \frac{\partial u_i}{\partial x_j}\right) = \frac{1}{\rho}\frac{\partial p}{\partial x_i} + g_i + f_i \tag{4}$$

where $u_i$ represents the velocities in the $x_i$ directions which are $x$, $y$, $z$-directions; $t$ is time; $A_i$ is the fractional area open to flow in the subscript directions; $V_F$ is the volume fraction of fluid in each cell; $\rho$ is fluid density; $p$ is hydrostatic pressure; $g_i$ is gravitational acceleration in the subscript directions; and $f_i$ represents the Reynolds stresses for which a turbulence closure model is required. To numerically solve a rapidly varying flow past a sluice gate, it is important that the free surface is accurately tracked. In FLOW-3D, the free surface is defined in terms of the volume of fluid (VOF) function $F$, which represents the volume of fraction occupied by the fluid. A two-equation renormalized group theory model (RNG model), as outlined by Yakhot and Orszag (1986) and Yakhot and Smith (1992), was used for turbulence closure. The RNG model is known for an accurate description of low intensity turbulence flows and flows having strong shear regions.

The computational domain is subdivided using Cartesian coordinates into a grid of variable-sized hexahedral cells. For each cell, average values for the flow parameter, that is, pressure and velocity, are computed at discrete times using a staggered grid technique. The staggered grid places all dependent variables at the center of each cell except for the velocities and the fractional areas. Velocities and fractional areas are located in the center of the cell faces normal to their associated direction. Most terms in the equations are evaluated using the current time-level values of the local variables, i.e., explicitly, although various implicit options exist as well. This produces a simple and efficient computational scheme for most purposes but requires a limited time-step size to maintain stable and accurate results.

One important exception to this explicit formulation is the treatment of pressure forces. Pressures and velocities are coupled implicitly by using time-advanced pressures in the momentum equations and time-advanced velocities in the continuity equation. This semi-implicit formulation of the finite difference equations allows for an efficient solution of low speed and incompressible flow problems. The semi-implicit formulation, however, results in coupled sets of equations that must be solved by an iterative technique. In FLOW-3D, two such techniques are provided. The simplest is a successive over-relaxation (SOR) method. In some instances, where a more implicit solution method is required, a special alternating direction, line implicit method (SADI) is available. In this study, SADI was used.

Two-dimensional numerical modeling (unit layer in $y$-direction) is carried out as shown in Fig. 2. The dimensions of the modeling region are $26a$ long and $12a$ high. To speed up convergence to a steady state solution, a manual multi-grid method was implemented. The use of an initial coarse grid allowed for a quick approximate water surface and discharge enhancement. A sequential finer grid was then initialized by interpolating the previous calculated values onto the grid. Starting the new grid with the old values allows the new solution to converge more quickly. A final orthogonal grid in which $0.025 \leq \Delta x/a \leq 0.265$ and $0.025 \leq \Delta z/a \leq 0.070$ was used. Fluid of 20°C was considered.
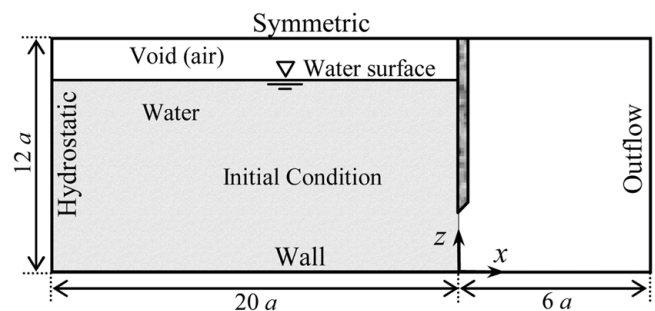


Fig. 2. Dimensions of Modeling Region Including Initial and Boundary Conditions

The boundary conditions of a given flow are as shown in Fig. 2, namely: upstream hydrostatic pressure; downstream outflow; bottom blocked by obstacle below (no slip); and top symmetry (no influence in this case because of gravity). The sluice gate boundary was modeled as a surface without slip. A $0.2a$ thick sluice gate was used, of which the crest was sharp-edged with a 45° bevel. With this configuration, the flow moves from left to right between the no slip floor and the atmospheric pressure boundary at the top. No slip is defined as zero tangential and normal velocities. Typically, these boundary conditions are set using so called "wall functions". That is, it is assumed that a

logarithmic velocity profile exists near a wall to compute an effective shear stress along the wall. Wall shear stresses are thereby applied to the obstacle surface using local Reynolds numbers and a algorithm taking into account the available fractional flow area (Flow Science, 2002). The experimental channel and the gate are generally made of PVC, glass, or steel, and hence its surface roughness height is around 0.05 mm (Hager, 1999).

The upstream boundary condition can be computed with one of the two pressure boundary conditions, static and stagnation. For the hydrostatic stagnation condition, $p_{bc}=E_1$ with $V_1=0$, and for the static condition, $p_{bc}=h_1$ with $V_1\neq0$. In some applications, the approach flow velocity may be insignificant and therefore omitted. In this study, the hydrostatic stagnation condition was used. The gate opening rate, $a/E_1$ ranged from 0.1 to 0.6 as upstream boundary conditions. In this study, $a$=5.0cm was adopted as the gate opening, because effects of viscosity are significant for $a$<5.0cm realizing in scale effects (Roth and Hager, 1999).

The initial condition was set such that a volume of fluid with an energy head $E_1$ was located at $x$=0. A transient flow analysis was carried out for a total time period of 100 s, when a steady state was reached. This was determined by inspecting results such as the kinetic energy and the turbulence kinetic energy of the system.

## 3. Results

### 3.1 Flow Characteristics

The simulated velocity fields near the sluice gate for $a/E_1$ = 0.2 and 0.5 are shown in Fig. 3. Accordingly, the velocity distribution is almost uniform both upstream and downstream of the gate and the velocity increases significantly near the gate opening. The results accurately simulated the underflow of a sluice gate with a typical stagnation region at the upstream surface and the transition from the subcritical upstream to the supercritical downstream gate flow forced by the presence of the gate. The results are used for further analysis of the gate flow features.

### 3.2 Contraction and Discharge Coefficient

The water surface profiles downstream of the gate were

calculated as shown in Fig. 3 and the contraction coefficients were determined using the computed flow depth at the vena contracta. The contraction coefficients from the present numerical analysis were compared with the existing experimental data in Fig. 4. Some recent experimental data and theoretical inviscid curves are also plotted in Fig. 4 for the sake of comparison. The contraction coefficients from the present analysis range from 0.618 to 0.630. The computed values of the contraction coefficient are slightly higher than the experimental results, a reasonable feature when considering the scatter of the experimental data in Table 2. The trend of the calculated contraction coefficients for the inviscid fluid flow was quite different from the experimental data, as shown in Tables 1 and 2. However, it can be seen from Fig. 4 that the contraction coefficient for the present study gradually decreases for $a/E_1$<0.4 and increases if $a/E_1$>0.4 with increasing $a/E_1$, exhibiting a tendency similar to that reported by existing experimental data (Benjamin, 1956; Rajaratnam and Subramanya, 1967) under the similar gate openings. For $a$<0.5cm, effects of viscosity are significant, realizing in a scale effect (Roth and Hager, 1999). For $a/E_1$<0.4, the trend corresponds to the theoretical solution of inviscid fluid; however, at higher values, the trend changes. This is considered to be a result of energy losses, particularly for $a/E_1$ is larger than 0.4. Fig. 5 shows the water surface profiles
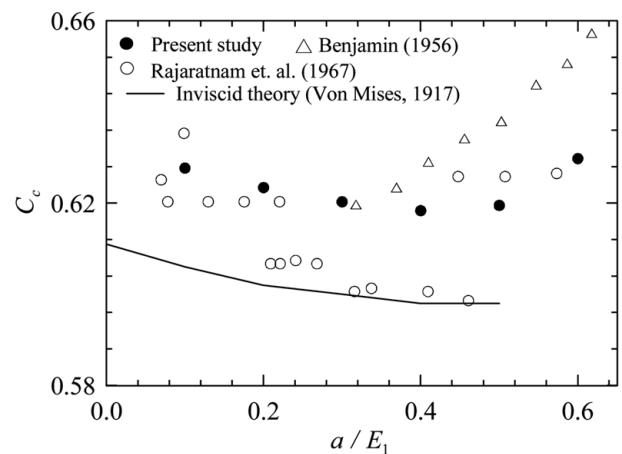


Fig. 4. Comparison of Contraction Coefficient from Present Analysis with Experimental Data
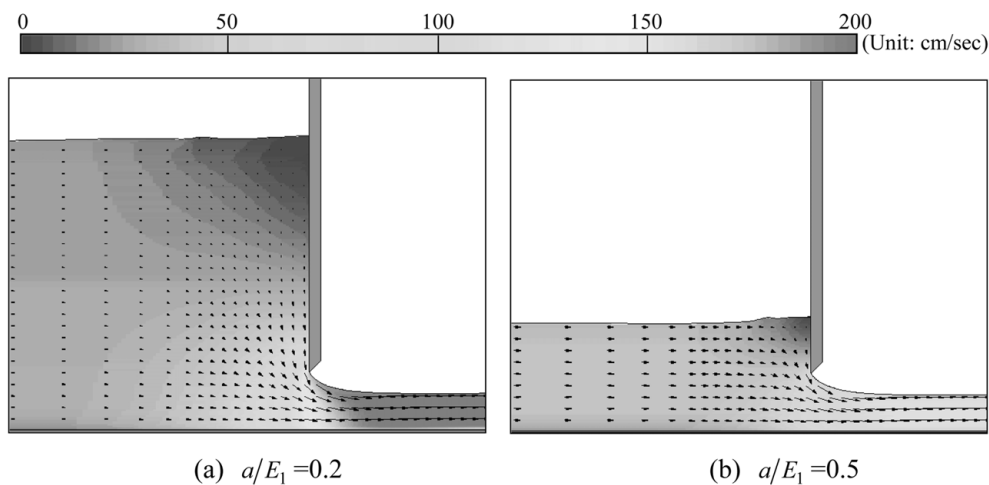


(a) $a/E_1$ =0.2      (b) $a/E_1$ =0.5

Fig. 3. Simulated Flow Fields Near the Sluice Gate
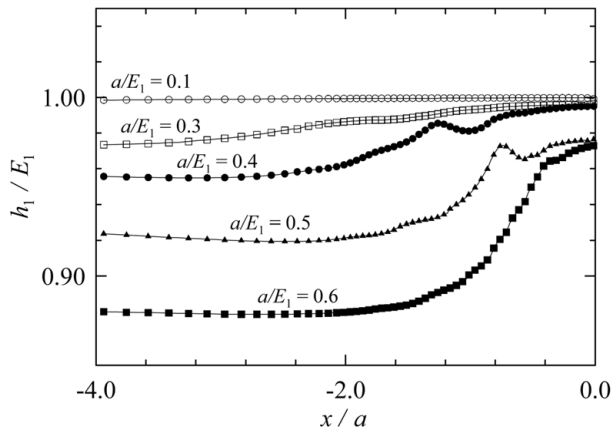
Fig. 5 Water Surface Profile Upstream from the Gate



Fig. 6. Pressure Profiles Along the Bottom

Table 4. Summary of the Discharge Coefficients from the Present Numerical Analysis

| $a/E_1$ | q (cm$^3$/s/cm) | $E_1$ (cm) | $h_1$ (cm) | $C_d$ |
|---|---|---|---|---|
| 0.1 | 934.26 | 50.00 | 49.82 | 0.598 |
| 0.2 | 634.34 | 25.00 | 24.66 | 0.577 |
| 0.3 | 496.45 | 16.67 | 16.19 | 0.557 |
| 0.4 | 412.37 | 12.50 | 11.89 | 0.540 |
| 0.5 | 351.20 | 10.00 | 9.27 | 0.521 |
| 0.6 | 306.38 | 8.33 | 7.48 | 0.506 |

upstream of the gate. As $a/E_1$ increases, the approach velocity head also increases and the energy losses increases greatly for $a/E_1>0.4$. Also, when $a/E_1>0.4$, the water surface profile changes rapidly upstream of the gate. The resultant water surface oscillationw were also considered to be the cause of the increased energy loss. Hence, the potential flow theory is limited for the analysis of free flow past a sluice gate to $a/E_1<0.4$.

The discharge coefficients from the present numerical analysis are summarized in Table 4. In Table 4, $q$ is determined as part of the solution, $h_1$ is determined by using the continuity and energy equations, and the discharge coefficients are calculated by using Eq. (2). The discharge coefficients from the present analysis range from 0.506 to 0.598. The results of the experimental data are very close to the existing experimental data, as shown in Table 3.

### 3.3 Bottom Pressure Distributions

The bottom pressure head, $h_p$, calculated by dividing the simulated hydrostatic pressure on the channel bottom by the specific water weight, varies along the channel from $h_p= h_1$ far upstream from the gate section to $h_p= h_3$ sufficiently downstream from the gate section. In this analysis, $h_1$ and $h_3$ were calculated at $x/a = $ - 5 and $x/a = 5$, respectively, where the pressure defect on the bed becomes negligible (Rajaratnam and Humphries, 1982). Fig. 6 refers to the following dimensionless bottom pressure head, $H_p$, as a function of dimensionless location, $x/a$

$$H_p = \frac{h_p - h_3}{h_1 - h_3} \qquad (5)$$

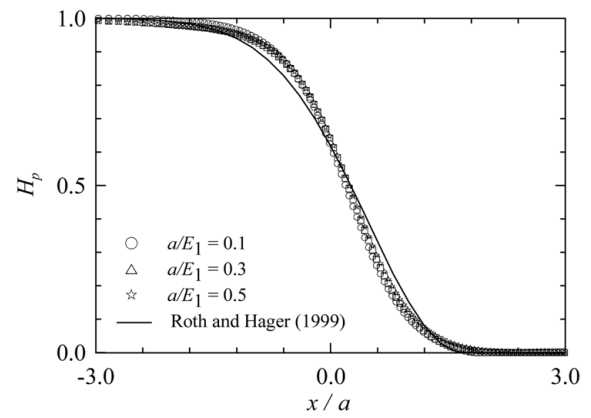The simulated pressure profiles along the bottom agree well

with the best fit curve of the experimental data of Roth and Hager (1999). Fig. 6 shows that the location of the steep pressure head gradient is close to $x/a$=0 and that the effect of non-hydrostatic pressure is confined to $-2<x/a<+2$. The bottom pressure immediately under the gate, $H_p(0)$, is about 0.63; interestingly, this is close to the critical flow depth of open channel flow. Considering that the regression curve of Roth and Hager (1999) slightly underestimates their experiment data upstream of the gate and overestimates at downstream, it can be seen that the modeling results of this study accurately reflect their data.

### 3.4 Gate Pressure Distributions

Fig. 7 shows the dimensionless gate pressure distribution $H_{pg}=h_{pg}/(E_1-a)$ as a function of dimensionless flow depth $Z = (z-a)/(E_1-a)$, where the pressure head on the gate, $h_{pg}$, is calculated by dividing the simulated hydrostatic pressure on the gate by the specific weight of water. In Fig. 7, $H_{pgM}$ is a dimensionless maximum pressure head. The best fitting curve of Roth and Hager's experimental data is also presented for comparison. The calculated pressure profiles on the gate agree well with those of Roth and Hager (1999). The pressure head is less than 0 at $Z$=1 when $a/E_1$=0.5 and 0.6 because of energy losses, as confirmed in Fig. 5.
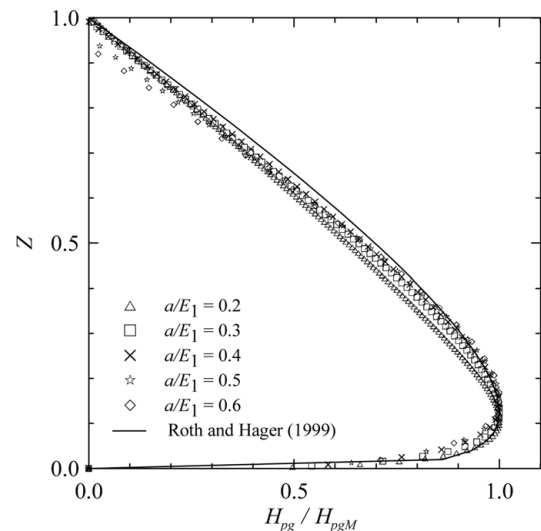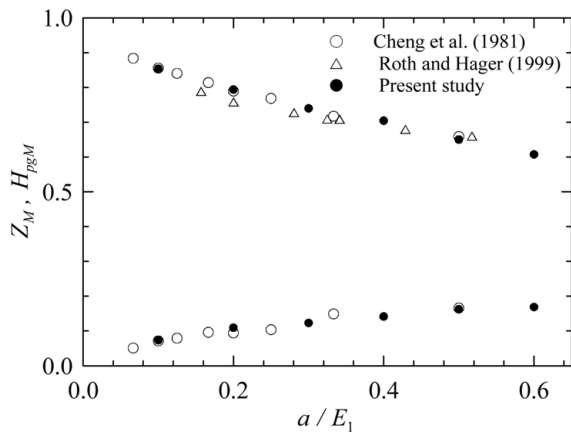


Fig. 7. Pressure Profiles on the Gate

Fig. 8. Dimensionless Maximum Pressure Head and its Vertical Location

The maximum pressure value on the gate, $H_{pgM}$, and its vertical location, $Z_M$, are shown in Fig. 8, showing good agreement with the measurement data of the maximum pressure of Cheng et al. (1981) and Roth and Hager (1999). The vertical location of the maximum pressure head increases with $a/E_1$, as found by Cheng et al. (1981).

## 4. Conclusions

This study shows that numerical tools using the RANS equations are sufficiently advanced to calculate the contraction and the discharge coefficients, and the pressure distribution for a free flow past a sluice gate. No assumptions regarding free surface geometry, real fluid flow, and gravity were introduced herein. In general, the experimental contraction coefficients are somewhat larger that those computed from potential flow theory, as shown in Tables 1 and 2. There is a continuous decrease of contraction coefficient as $a/E_1$ increases, a trend opposite to the experimental data. It can be seen from Fig. 4 that the contraction coefficient for the present study gradually decreases for $a/E_1 < 0.4$ and increases for $a/E_1 > 0.4$ as $a/E_1$ increases, exhibiting a tendency similar to existing experimental data. Fig. 5 confirms that this is a result of energy losses and an increase in water surface oscillation as the velocity head upstream of the gate increases when $a/E_1 > 0.4$. The discharge coefficients from the present analysis range from 0.506 to 0.598, i.e., close to the existing experimental data. The pressure distribution along the channel bottom and along the gate was also calculated, and similarly appear to be in good agreement with the data.

## Acknowledgement

## References

Benjamin, T.B. (1956). "On the flow in channels when rigid obstacles are placed in the stream." *J. Fluid Mech.*, Vol. 1, pp. 227-248.

Cheng, A.H.D., Liggett, J.A., and Liu, P. (1981). "Boundary calculations of sluice and spillway flows." *J. Hydraulics Div.*, ASCE, Vol. 107, No. 10, pp. 1163-1178.

Chung, Y.C. (1972). "Solution of flow under sluice gates." *J. Engineering Mech. Div.*, ASCE, Vol. 98, No. 1, pp. 121-140.

Fangmeier, D. and Strelkoff, T.S. (1968). "Solution for gravity flow under sluice gates." *J. Engineering Mech. Div.*, ASCE, Vol. 94, No. 1, pp. 153-176.

Flow Science, Inc. (2002). *FLOW-3D (theory manual)*, Los Alamos, NM.

Hager, W.H. (1999). *Wastewater hydraulics*, Springer, Berlin.

Henderson, F.M. (1966). *Open channel flow*, Macmillan, New York.

Isaacs, L.T. (1977). "Numerical solution for flow under sluice gates." *J. Hydraulics Div.*, ASCE, Vol. 103, No. 5, pp. 473-481.

Larock, B.E. (1969). "Gravity affected flows from planar sluice gates." *J. Hydraulics Div.*, ASCE, Vol. 95, No. 4, pp. 851-864.

Lin, C.H., Yen, J.F., and Tsai, C.T. (2002). "Influence of sluice gate contraction coefficient on distinguishing condition." *J. Irrigation and Drainage Eng.*, ASCE, Vol. 128, No. 4, pp. 249-252.

Masliyah, J.H., Nandakumar, K., Hemphill, F., and Fung, L. (1985). "Body fitted coordinates for flow under sluice gates." *J. Hydraulic Eng.*, ASCE, Vol. 111, No. 6, pp. 922-933.

Montes, J.S. (1997). "Irrotational flow and real fluid effects under planar sluice gates." *J. Hydraulic Eng.*, ASCE, Vol. 123, No. 3, pp. 219-232.

Rajaratnam, N. and Humphries, J.A. (1982). "Free flow upstream of vertical sluice gates." *J. Hydraulic Research,* IAHR, Vol. 20, No. 5, pp. 427-437.

Rajaratnam, N. and Subramanya, K. (1967). "Flow equation for the sluice gate." *J. Irrigation and Drainage Eng.*, ASCE, Vol. 93, No. 3, pp. 167-186.

Roth, A. and Hager, W.H. (1999). "Underflow of standard sluice gate." *Experiments in Fluids*, Vol. 27, pp. 339-350.

Savage, B.M. and Johnson, M.C. (2001). "Flow over ogee spillway: Physical and numerical model case study." *J. Hydraulic Eng.*, ASCE, Vol. 127, No. 8, pp. 640-649.

Vanden-Broeck, J.M. (1997). "Numerical calculations of the free surface flow under a sluice gate." *J. Fluid Mech.*, Vol. 330, pp. 339-347.

Yakhot, V. and Orszag, S.A. (1986). "Renormalization group analysis of turbulence. I. Basic theory." *J. Scientific Computing*, Vol. 1, No. 1, pp. 1-51.

Yakhot, V. and Smith, L.M. (1992). "The renormalization group, the ε-expansion and derivation of turbulence model." *J. Scientific Computing*, Vol. 7, No. 1, pp. 35-61.